

Provided for non-commercial research and education use.
Not for reproduction, distribution or commercial use.



This article appeared in a journal published by Elsevier. The attached copy is furnished to the author for internal non-commercial research and education use, including for instruction at the authors institution and sharing with colleagues.

Other uses, including reproduction and distribution, or selling or licensing copies, or posting to personal, institutional or third party websites are prohibited.

In most cases authors are permitted to post their version of the article (e.g. in Word or Tex form) to their personal website or institutional repository. Authors requiring further information regarding Elsevier's archiving and manuscript policies are encouraged to visit:

<http://www.elsevier.com/copyright>



ELSEVIER

Journal of Environmental Management 90 (2009) 2189–2198

 Journal of
**Environmental
 Management**

www.elsevier.com/locate/jenvman

Exploring the capacity of radar remote sensing to estimate wetland marshes water storage

F. Grings^a, M. Salvia^a, H. Karszenbaum^a, P. Ferrazzoli^{b,*}, P. Kandus^c, P. Perna^a

^a Instituto de Astronomía y Física del Espacio (IAFE), Ciudad Universitaria, 1428 Buenos Aires, Argentina

^b Università di Roma "Tor Vergata", Facoltà di Ingegneria, Dipartimento di Informatica, Sistemi e Produzione (DISP), Via del Politecnico 1, 00133 Roma, Italy

^c Universidad de Buenos Aires, Facultad de Ciencias Exactas y Naturales (FCEyN), Departamento de Ecología, Genética y Evolución, Laboratorio de Ecología Regional, Ciudad Universitaria, Pab. II, 1428 Buenos Aires, Argentina

Received 24 October 2006; received in revised form 2 March 2007; accepted 26 June 2007

Available online 25 March 2008

Abstract

This paper focuses on the use of radar remote sensing for water storage estimation in wetland marshes of the Paraná River Delta in Argentina. The approach followed is based on the analysis of a temporal set of ENVISAT ASAR data which includes images acquired under different polarizations and incidence angles as well as different environmental conditions (water level, precipitation, and vegetation condition). Two marsh species, named *junco* and *cortadera*, were monitored. This overall data set gave us the possibility of studying and understanding the basic interactions between the radar, the soil under different flood conditions, and the vegetation structure. The comprehension of the observed features was addressed through electromagnetic models developed for these ecosystems. The procedure used in this work to estimate water level within marshes combines a direct electromagnetic model, field work data specifically obtained to feed the model, the actual ASAR measurements and a well known retrieval scheme based on a cost function. Results are validated with water level evaluations at specific points. A map showing an estimation of the water storage capacity and its error in *junco* and *cortadera* areas for the date where the investigation was done is also presented. © 2008 Elsevier Ltd. All rights reserved.

Keywords: Remote sensing; Radar; Wetland marshes; Water storage

1. Introduction: problem statement

In the Lower Delta of the Paraná River in Argentina, marshes are the most extended autochthonous vegetation. Two main species dominate the marsh vegetation: *junco* (*Shoenoplectus californicus*) and *cortadera* (*Scirpus giganteus*), which together cover up to 45% of the area (about 800 km²) (Kandus et al., 2003). These marshes are responsible for the water buffer effect on this wetland, a key phenomenon in flood and storm control and a key argument in wetlands

conservation policies. In order to fully understand this buffer effect, it is important to measure and monitor the water storage capacity of the marsh, that is, the volume of water that a marsh can accept in a given marsh area.

This topic is not only a regional issue but a global one: wetlands cover up to 5% of the earth's land surface, and inside them, major biogeophysical processes take place. The most dynamic of these processes is water exchange between the wetland and the river basin. Furthermore, large fluctuations in water levels are certainly the rule in natural watersheds. In most of the major river watersheds, the average flux of water between seasons increases up to ten times or more (Keddy, 2002). In the Amazon basin, for example, the water level changes up to 10 m between seasons in a surface of 700 000 km² (Junk et al., 1989). In other cases, variations are of the order of a few centimeters. Furthermore, almost no stage

* Corresponding author.

E-mail addresses: verderis@iafe.uba.ar (F. Grings), msalvia@iafe.uba.ar (M. Salvia), haydeek@iafe.uba.ar (H. Karszenbaum), ferrazzoli@disp.uniroma2.it (P. Ferrazzoli), pato@ege.fcen.uba.ar (P. Kandus), pperna@iafe.uba.ar (P. Perna).

recording devices are located on any of the world's large, low-land floodplains. Instead, discharge is measured only in the main channels where flow is confined, unlike floodplains, where flow is unrestricted. This can be explained partially by the fact that many wetlands (Paraná River wetlands among them) are fragmented ecosystems that are effectively subdivided in different patches separated by island levees (Kandus et al., 2003). Therefore, it is very difficult to measure water level using conventional means (measure water level in point locations). Remote sensing radar systems are the only tools that have the potential to systematically monitor water level inside marshes at regional scale (Bach and Mauser, 2003).

It is important to mention that it is a common practice to estimate floodplain storage values *assuming* that floodplain water levels and their temporal fluctuations are equivalent to those of the main river channel. Several field measurements suggest that this assumption may not be justified in fragmented ecosystems (Pratolongo, 2005; Keddy, 2000). For example, Alsdorf (2002) reported that the difference between assumed floodplain storage change values and an estimate using SAR interferometry is about 30%. Furthermore, Coe (2000) reported that a wetland component could provide up to 50% of the observed Nile River discharge in the Sudan, and Richey et al. (1989) estimated that the Amazon floodplain-to-mainstream flux is about 25% of the annual discharge. These large percentages suggest that inaccurate knowledge of floodplain storage and subsequent discharge can lead to significant errors in hydrological, sediment flux, and biogeochemical models (Alsdorf, 2002).

Although it is accepted that a remote sensing approach is the only method to systematically monitor water level inside large marshes, there is still some discussion about the sensors and the techniques to be used. Radar altimetry is a profiling tool with a satellite track spacing of ~ 300 km, thus, it misses significant portions of a floodplain. Inferring floodplain storage and discharge from inundated areas require calibration with ground discharge data and does not work well in environments where small changes in water heights yield small changes in surface area but significant changes in flow (Alsdorf, 2002). Another recently developed approach to measure water level inside marshes at a centimeter scale is the use of InSAR techniques (Sang-Wan et al., 2005; Alsdorf, 2002). The images required, the techniques used and the drawbacks of the method are concisely described in the comprehensive review by Alsdorf (2002). Although this method presents an outstanding capability for water level retrieval inside marshes (Sang-Wan et al., 2005), it requires: (1) an interferometric pair for every water level estimation, and (2) stable scatterers to preserve coherence (Sang-Wan et al., 2005). These facts limit the operational implementation of this technique.

The technique explored in this work to monitor water level below marshes (Grings et al., 2006) consists of characterization of marsh parameters from field work for a given date, measure or model the time variation of these parameters, use an electromagnetic model to simulate the radar response of the marshes present in the Lower Paraná Delta (*junco* and *cordadera*) and combine simulations and observations in a water

level retrieval scheme produced for each marsh type (structure) considered. Furthermore, the capacity of the ENVISAT ASAR instrument to estimate differences in water level within these marshes is exploited by generating a map of the marsh area showing the spatial distribution of water levels below the vegetation. Although this type of maps are very difficult to validate due to the lack of measurements of water level within the floodplain, sources of errors are discussed as well as the importance of such a map for hydrological modeling and floodplain monitoring.

Section 2 briefly refers to well known papers on radar and wetlands, and our previous work in this subject emphasizing recent papers where the use of electromagnetic models permitted a considerable improvement in information extraction from radars.

2. SAR response in wetlands

The synthetic aperture radar (SAR) instrument is an active sensor onboard satellites that acquires data of the earth surface in the microwave region of the electromagnetic spectrum. In particular, in wetlands, it is capable of providing information about vegetation structure and hydrological conditions. The presence or absence of water (which has a much higher dielectric constant than dry or wet soil) in wetlands may significantly alter the signal detected from these areas depending on the dominant vegetation type, its density and height. Several authors have already investigated the characteristics of the backscattering coefficient σ^0 at various frequencies and polarizations for different types of wetland marshes. Among the relevant ones, we can mention the works of Pope et al. (1997), Kasischke et al. (2003), and Hess et al. (1995). The first one analyzed SIR-C polarimetric radar imagery of wetlands in Central America, and the main conclusions were that water under vegetation could be detected by an increase or a decrease of σ^0 : increase in marshes with mainly vertical orientation, decrease in short, randomly oriented marshes. In the first case, the increase in HH is greater than in VV. Kasischke et al. (2003) presented comparable results analyzing the radar backscatter measured from ERS-2 imagery in Florida (USA) wetlands. Hess et al. (1995) showed how it is possible to accurately delineate inundation and different vegetation types using multifrequency polarimetric radar (SIR-C) along the Amazon floodplain.

This paper addresses a large region of marshes in Argentina which was observed by different SAR systems. Parmuchi et al. (2002), discussed RADARSAT-1 data that were acquired during 1998 El Niño event. Inundated areas were mapped using supervised and unsupervised procedures based on multitemporal images that combined two extreme episodes, normal flood conditions and extreme floods (vegetation covered by water). Karszenbaum et al. (2000) compared observations of HH and VV polarizations using two SAR systems, RADARSAT-1 and ERS-2, in two types of marshes and in forests.

Recently, electromagnetic models were introduced to further exploit and benefit from radar data capabilities. They consist of algorithms that simulate the wetland radar response by obtaining the coefficient of backscattering σ^0 for vegetation

and soil under different environmental conditions (flooded, non-flooded, burn vegetation, others). Vegetation elements are modelled as simple objects (shoots as cylinders, leaves as disks). The model used here, developed at Tor Vergata University, is able to simulate the marsh σ^0 under various environmental conditions (details on the model can be found in Section 6). By comparing simulated backscattering coefficients with observed ones, the electromagnetic model can be validated. Once the model is validated, it can be used, in conjunction with ground truth data, to develop a retrieval scheme. In this way, the combination of observations, models and field work allows us to develop and test retrieval algorithms (i.e., an algorithm to monitor flood condition within marshes). In this line of work, Grings et al. (2005) introduced EM models for *junco* marshes and successfully explained an ERS-2 VV multi-temporal data set that showed the re-growth of *junco* marsh patches after an intense burn, based on restricted scattering and biophysical assumptions. More recently, we used two versions of the model (Grings et al., 2006) to interpret the radar response (VV and HH) of *junco* and *cortadera* marshes on occasion of an extraordinary flooding event observed with ENVISAT ASAR APP S1 mode.

Radar data, provided through ESA ENVISAT ASAR AO 667 project, includes observations of the Paraná River Delta marshes under different environmental conditions using HH, VV and HV polarizations, and steep and slant incident angles.

This work shows the capabilities of these data to monitor flood condition within wetlands and explores how the combination of radar observations of different polarizations, electromagnetic models and field data could be used to determine the water storage in marshes of known structure.

3. Study site: hydrology and vegetation structure

The Paraná River Delta (PRD) region stretches through the final 300 km of the Paraná basin. It covers approximately 17 500 km², close to Buenos Aires city in Argentina (Fig. 1). The Paraná River drains an approximate area of 2 310 000 km² and, according to its length, basin size, and water discharge, is considered the second most important in South America after the Amazonas. Among the great rivers throughout the world, it is the only one that flows from tropical to temperate latitudes, where it joins the Uruguay River ending in the Del Plata estuary.

The landscape patterns of this region are subordinated to a flooding regime characterised by different sources of water with a different behaviour, that is, local precipitation, and large rivers whose specific flooding patterns affect particular areas. Sometimes these sources add together provoking large flooding events. The greatest influence comes from the Paraná River, which shows a main flood peak in late summer and a second peak in winter. The final portion is also influenced

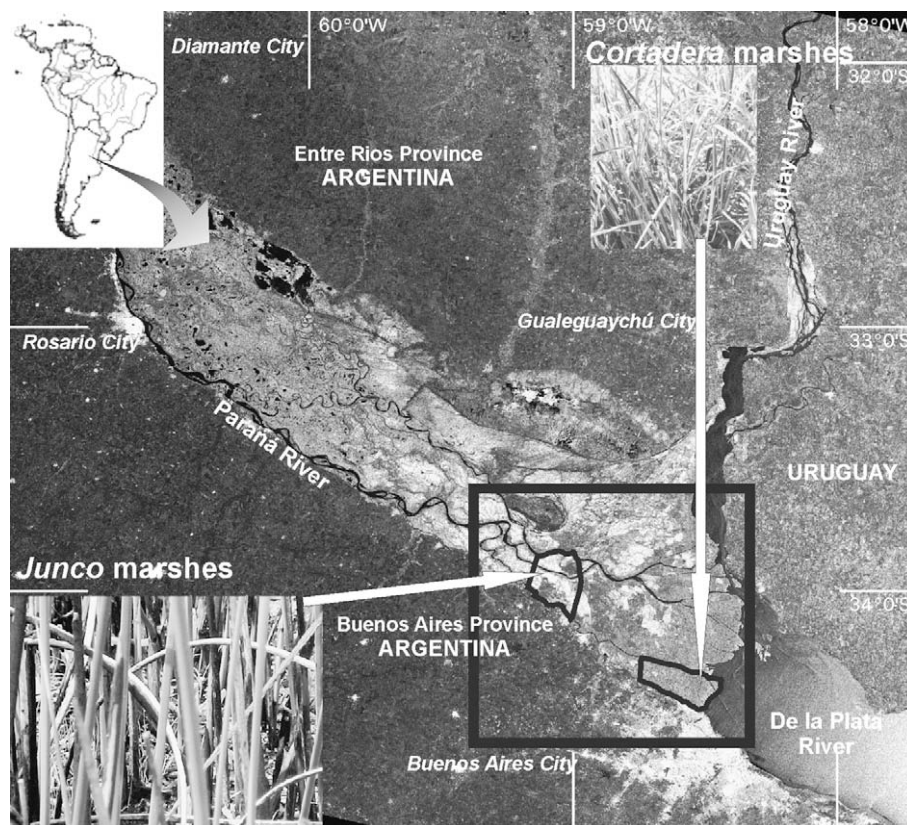


Fig. 1. ENVISAT ASAR wide scan mode (WSM) HH polarization image of the Paraná River Delta area acquired in September 2006 (pixel size: 75 m). Buenos Aires city can be observed in the lower right portion. Black square indicates study area and black polygons show areas where field work was done. Top right photograph corresponds to *cortadera* marshes and bottom left to *junco* marshes.

by the De La Plata River with its daily wind and lunar tides. The combined effects of wind and tide result in frequent but short (hours-long or day-long) floods.

The combination of local topographic gradients and a regional flooding regime constitutes the primary factor that determines the emergent natural vegetation, consisting of marshes growing in lowlands where the substrate is saturated or flooded either during long periods or permanently (Kandus, 1997). Conversely, forests are restricted to levees and other areas where soils are generally dry or flooded only during wind tides and (or) fluvial floods. It is important to look at the soil condition, because this condition may be modified by high water levels caused by the dynamics of the different river regimes (specially the Paraná and the De la Plata).

This paper focuses on the area of the lower portion of the PRD, which covers 2700 km², and is formed by typical pan-shaped islands with perimetrical levees and a central depression. Island elevations vary between 0.5 and 3 m above sea level. In this area, we consider two marsh types, *junco* and *cortadera*:

- (a) the *cortadera* marshes are dominated by *Scirpus giganteus*, which is a perennial rhizomatous species that grows through the repeated production of ramets, and emergent structures develop at nodes located in rhizomes, below the ground surface. Shoots are not visible in vegetative ramets and the long leaves (with average LAI equal to about 5) are the only observable structures of mats. Only in flowering mats, shoots lengthen to 1 m or taller and spikelets develop at the tip of the stem. *Scirpus giganteus* produces new ramets throughout the year (Pratolongo, 2005). This species shows a stable inter-annual behavior. *Cortadera* marsh patches have nearly uniform vertical density and a average height of 2 m. They are located in the inner portion of the delta islands, near the deltaic front. Eight marsh fields have been analyzed in this work
- (b) The *junco* marshes are placed in permanently flooded soils and are dominated by *Schoenoplectus californicus*, a perennial reed up to 2.5 m tall, with culms developing at nodes located in creeping rhizomes and leaves reduced to bladeless sheaths at the base of culms. It is a patchy ecosystem that not only shows seasonal variations but also annual and inter-annual fluctuations in standing biomass probably due to frequent fire events (Pratolongo, 2005). Most fires are intentional for wildlife hunting activities or just to prevent dried biomass accumulation. *Junco* marsh patches look like arrangements of long, nearly vertical, cylinders that range from young stands (height = 25 cm, density = 10 m⁻²) to mature stands (height = 200 cm, density = 60 m⁻²). They are also located in the inner portion of the islands, but these islands are located about 50 km upstream the Paraná River.

4. Radar data and field work

This work uses ENVISAT ASAR precision image products in alternating polarization mode (AP). For each date, there is

a multi-look ground range digital image. Data are similar to image mode products, but include a second image acquired using a second polarization combination. The polarizations used are: the co-polarized sub-mode HH/VV. This mode can be acquired under different incidence angles (ESA, 2006).

With the objective of describing and simulating *junco* and *cortadera* marsh radar signatures, for several flood conditions, incidence angles, and polarizations, in 2004 we started to use a detailed field work methodology simultaneously with ENVISAT data acquisitions. Field methods were adapted from previous works. Five quadrates of 50 × 50 cm² were established in each of two stands representative of *S. californicus* marsh (*junco* marsh). After counting stems inside the plots, and measuring water level, a complete harvesting and weighting of plant material was performed. In the laboratory, the collected material was rinsed, and diameter and length of each stem was measured. All collected material was dried for 72 h at 60 °C and weighted. Mean stem biomass (green and dead) per quadrant and per sampling period was estimated as well as gravimetric and volumetric moisture content. This was repeated for subsequent satellite data acquisition. For an estimate of water level inside marshes, rivers' water table and precipitation data were used.



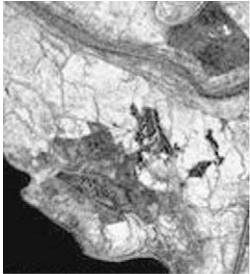





The same method was used for *cortadera* marshes, with the exception that for *cortadera* ramets, LAI (leaf area index) and leaf longitude were measured for each leaf, and height was measured for the ramet as one; and biomass was measured per quadrate and per ramet.

5. Water level below marshes

The lower delta of Paraná River has been observed by various spaceborne SARs (RADARSAT-1, ERS-2 and ENVISAT ASAR) since 1997. This data set covers from average water level conditions to strong floodings due to El Niño event of 1998. Table 1 presents two key evidences on how SAR response changes with water level and marsh species. The first line describes an El Niño event illustrated by multitemporal RADARSAT-1 HH images before and during the flood. The second line shows how the combination of ENVISAT ASAR HH/HV and ERS-2 VV images is able to discriminate among vegetation species.

More recently, ENVISAT ASAR observed a simultaneous tidal and fluvial flooding event. This episode gave us the opportunity to observe both marshes during different, nonextreme, flooding conditions. As expected, water level changes modified the radar response of both *junco* and *cortadera*. This is illustrated in Fig. 2a and b. This figure shows a multitemporal image that combines three different environmental conditions: red is associated to the October image (spring and normal water levels in rivers), green to the November image (spring and a strong increase in water level) and blue to the March image (beginning of autumn). At VV polarization (Fig. 2a) the wetland radar response is quite uniform, and does not show evidences of multitemporal changes. On the contrary, agricultural areas show a stronger response in the November image. At HH polarization (Fig. 2b) the wetland

Table 1
Evidences relating changes in σ^0 with changes in wetland surface hydrology and vegetation structure

Photographic evidence	SAR image	Evidence description	Evidence interpretation	Evidence exploitation
 	 	<p>Top photograph and top image show <i>junco</i> marshes in normal flood condition, as seen by RADARSAT-1 HH polarization.</p> <p>Bottom photograph and bottom image illustrate “El Niño” event of 1998, when <i>junco</i> marshes were covered by water.</p>	<p>When <i>junco</i> marshes are under normal condition (water in the soil) the main signal-target interaction mechanism is soil-shoot double bounce, and the <i>junco</i> σ^0 is high.</p> <p>When the water covers the <i>junco</i> marsh, only the water surface return (low σ^0) is observed.</p>	<p>A map was generated using a decision tree. The map delineates the flooded and non-flooded zones for <i>junco</i> marshes. It was evaluated using an error matrix scheme (Parmuchi et al., 2002).</p>
 	 	<p>Top photograph and top image show <i>junco</i> marshes, and bottom photograph and bottom image show <i>cortadera</i> marshes.</p> <p>The images shown correspond to a combination of an Envisat ASAR (HV in red, HH in green) and an ERS-2 (VV, in blue). These images clearly illustrate, how the σ^0 of <i>junco</i> and <i>cortadera</i> differs according to polarization.</p>	<p><i>Junco</i> and <i>cortadera</i> marshes are two herbaceous vegetations with a main vertical orientation. This implies that the main interaction mechanism present when soil is flooded is soil-shoot double bounce. In both <i>junco</i> and <i>cortadera</i>, the relation $HH \sigma^0 > VV \sigma^0$ is valid. HV σ^0 is low but nonzero for both marshes. The polarization effects provide important additional information.</p>	<p>An interaction model has been developed for both <i>junco</i> and <i>cortadera</i> (see Section 6) that simulates the marsh σ^0 for different environmental conditions. Using this model, the σ^0 of both marshes has been successfully simulated for different phenological conditions (Grings et al., 2006). The observed differences in polarimetric responses have been partially explained in Grings et al. (2006), and Grings et al. (in press).</p>

radar response shows important differences along the wetland area. On one hand, these are related to different vegetation covers. On the other hand, they are also due to temporal differences, which are related to distinct hydrological conditions at the acquisition times. These changes in the radar response can be attributed to the fact that the increase in water level reduces the amount of emerged biomass. Based on this, we proposed a vegetation-dependent flooding prediction scheme for two marsh structures: nearly vertical cylinders (*junco*-like) on flooded soils and randomly oriented discs (*cortadera*-like) also on flooded soils (Grings et al., 2006).

Fig. 3 shows a trend of backscattering coefficients as a function of time. The overpasses of November 20, 2003 and April

8, 2004 are included. For each overpass, the boxes indicate the average backscattering coefficient \pm the standard deviation and the range of measured values for all the observed samples (15 for *junco* marshes and 8 for *cortadera* marshes). The effect of a decrease in the water level below the marshes is different, depending on the polarization and the marsh type. At VV polarization (Fig. 3a), σ^0 in the flooded condition is generally higher than σ^0 in the non-flooded condition for both marshes, but this change is small. Nevertheless the differences in σ^0 at HH polarization between flooded and non-flooded conditions are much larger for both marshes (Fig. 3b). This effect has already been observed by other authors on similar marshes (Pope et al., 1997).

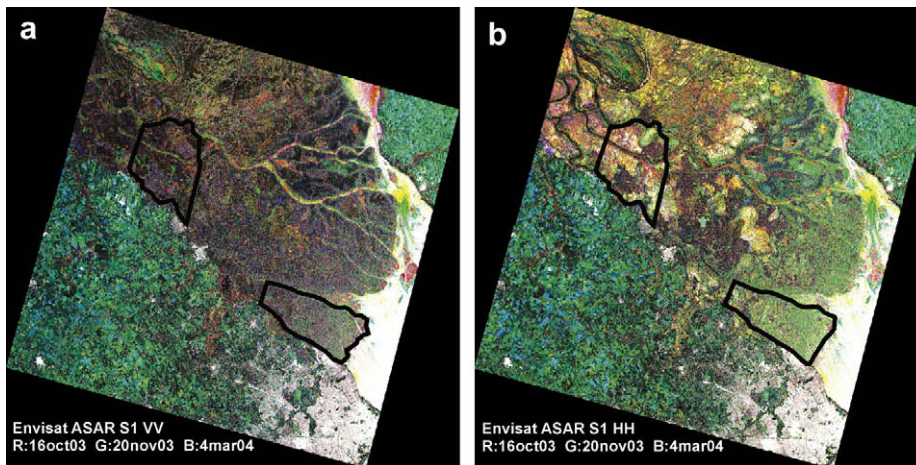


Fig. 2. (a) ENVISAT ASAR S1 VV multitemporal image (October, November, 2003, March 2004) and (b) ENVISAT ASAR S1 HH multitemporal image (October, November, 2003, March 2004). Test areas are indicated in black.

6. Exploiting observations using electromagnetic models

Changes in σ^0 can be related to changes in different environmental variables. In our case, large changes in σ^0 of *junco* and *cortadera* marshes can be related to changes in water level, plant geometry, plant spatial arrangement, phenology, and plant water content. But σ^0 can also be weakly related to changes in wind condition, plant salinity and floating vegetation. Therefore, an interaction model that simulates the σ^0 of marshes given the environmental variables that characterize them, is necessary to quantify the weight that each environmental variable has in the resulting σ^0 .

6.1. General aspects

The flood monitoring technique proposed in this paper requires to model and explain the effects of flooding events on the backscattering coefficient of considered marsh areas. To this aim, the scattering processes have been simulated by the electromagnetic model developed at Tor Vergata University (Bracaglia et al., 1995). In its general version, the model

describes the soil as a homogeneous half space with a rough interface and the vegetation as a discrete ensemble of lossy dielectric elements. Canonical shapes, such as discs and cylinders, are selected for the elements.

Junco marshes are normally flooded. Therefore, soil permittivity has been set equal to fresh water's one. Vegetation is dominated by near-vertical shoots, which are cylinders in our representation. A sketch is given in Fig. 4a. Since water surface is flat, the soil-shoot specular double bounce is the dominant effect, as it will be shown in next sections. Input variables for the *junco* model are based on ground measurements.

Cortadera marshes, under normal conditions, have a saturated soil, but it may be flooded during extreme events. Vegetation is dominated by wide and thick leaves, which are discs in our representation (see the sketch in Fig. 4b). The number of discs per unit area may be computed as the ratio between leaf area index (LAI) and single disc area. Input variables for the *cortadera* model, are also based on ground measurements. Details on the model and its input variables are given by Grings et al. (2006).

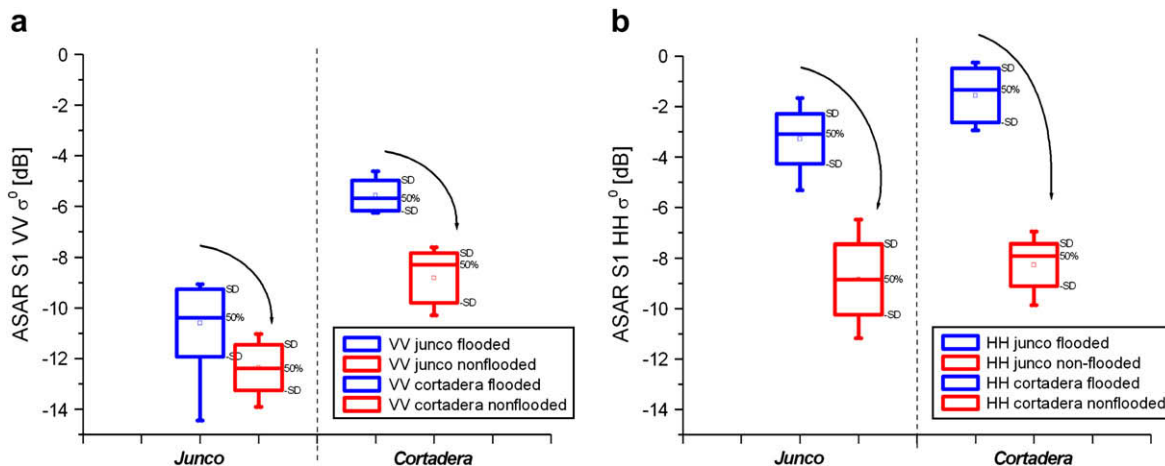


Fig. 3. Box plot diagrams resulting from ENVISAT ASAR S1 data collected over *junco* and *cortadera* marshes for two conditions. Blue: November 20 overpass, flooded marsh. Red: April 8 overpass, non-flooded. (a) VV polarization and (b) HH polarization.

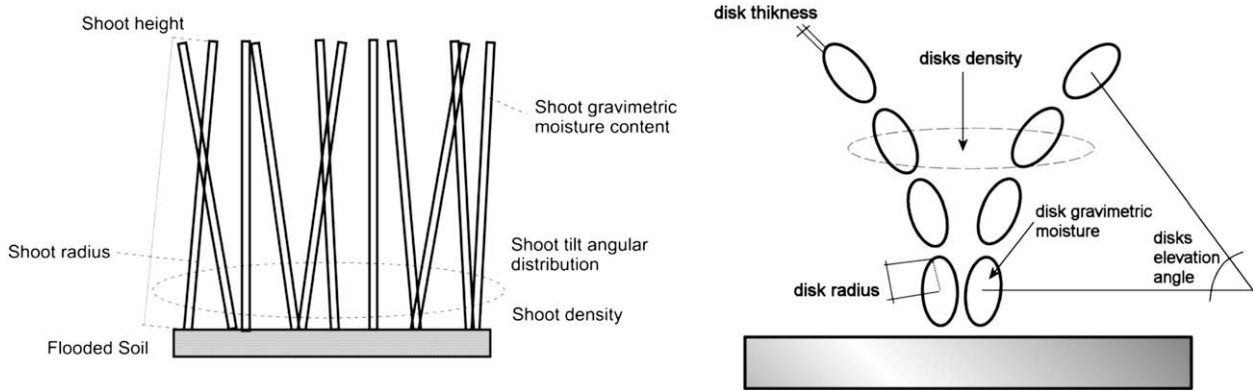


Fig. 4. Sketches of the marsh models adopted: (a) *junco* marshes model is constructed using nearly vertical cylinders and (b) *cortadera* marsh is modeled using random disks with a preferential tilt distribution.

6.2. Application to flooding

To correctly simulate the flooding event, we need to specify how an increase in water level affects the input variables in our model. This effect is different for different marshes. In the case of *cortadera*, our hypothesis is that observed changes in σ^0 are related to a reduction in the emerged biomass caused by the flood. This reduction in the emerged biomass implies a reduction in the “emerged LAI”.

Taking into account that:

- the vertical density of leaves can be considered as uniform,
- the angular distribution of *cortadera* leaves can be considered $U \sim [0-45^\circ]$,
- the non-flooded (maximum) *cortadera* LAI (LAI_{Max}) is constant,

we can relate the water level x to the emerged LAI as:

$$x = \left(1 - \frac{LAI}{LAI_{Max}}\right) h_c \quad (1)$$

where h_c is the *cortadera* height. Since *cortadera* height can be considered constant for this marsh, we can relate “emerged LAI” with water level inside the marsh.

In the case of the *junco*, the observed increase in σ^0 is related to a reduction of the emerged plant height caused by the flood. This effect was also reported by other authors in similar marshes (Pope et al., 1997). In this case, the water level (x) is related to shoots height in the simple form:

$$x = h_{Max} - h_j \quad (2)$$

where h_j is the emerged *junco* height and h_{Max} is the total *junco* height.

6.2.1. Water level retrieval scheme

For the observations of November 20 and April 8, which have been used in Fig. 3, the model has been run and model outputs have been used to test a water level retrieval algorithm for *cortadera* and *junco* sites. This was done by finding the best estimation for a given set of ASAR dual polarization

observations. Mathematically, this is done by minimizing the cost function:

$$CF = \sum_{m=1}^{Ms} \sum_{p=1}^2 \left[\sigma_{ppS}^0(WL) - \sigma_{ppM}^0 \right]^2 \quad (3)$$

where $\sigma_{ppS}^0(WL)$ is the simulated backscattering coefficient at pp polarization for WL water level, σ_{ppM}^0 is the backscattering coefficient at the same polarization collected by ASAR over the marsh field and Ms is the number of marsh fields within the site. In the way it is stated, this algorithm chooses the WL that performs the best fit of HH and VV simultaneously.

Finally, estimated water levels have been compared with measured water levels. Results are shown in Fig. 5. Of course, the two samples with low water level values correspond to non-flooded condition, while the two samples with higher water level values correspond to flooded condition. For *junco* marshes and flooded *cortadera* marshes there is a general agreement. For non-flooded *cortadera* a systematic error is observed. This is due to a model underestimation of direct vegetation scattering from *cortadera* leaves. Indeed, *cortadera*

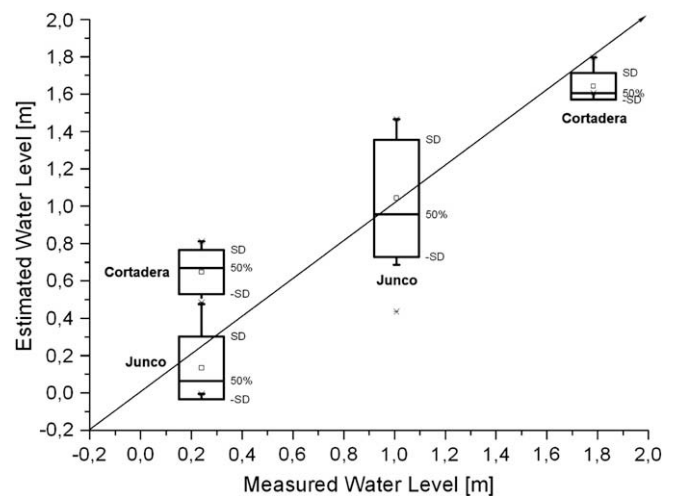


Fig. 5. Comparison between measured and estimated water levels inside *junco* and *cortadera* marshes. The estimated water level was obtained by minimizing the cost function (Eq. (3)).

leaves have a complex curved structure, which is only partially represented by the disc approximation. The overall *rms* error for water level estimation is 22 cm (Grings et al., 2006).

7. Estimation of marshes water storage capacity

Once the water level inside *junco* and *cortadera* marshes has been retrieved, an estimation of marsh water storage may be obtained. Using a land cover map of the PRD (Kandus, 1997), the area covered by specific marsh patches was determined. In order to estimate marsh water storage, a set of simplifying assumptions must be adopted:

- H.1 water level within a marsh patch surrounded by island levees is constant;
- H.2 vegetation structure (phenological condition) is statistically similar in different regions of a single patch;
- H.3 vegetation structure is statistically similar in different neighboring patches;
- H.4 there is no significant variation in the island surface height between island borders and island center (the island can be considered as a constant depth container).

Using these hypotheses, the water volumes inside *junco* and *cortadera* marshes in islands near the ones where we have done the field work have been estimated (Fig. 6).

In order to assign an error to the values reported in Fig. 6, the simplifying hypothesis must be analyzed carefully. H.1 is generally true, because marsh patches are small and have no large drain currents (Sang-Wan et al., 2005). H.2 is also generally true, because although marshes present a large spatial variability of biophysical variables, they change in a very small correlation length, much smaller than ASAR pixel size. So, taken the patch as a whole, the biophysical variables are roughly constant. Regarding hypothesis H.3, marsh patches mapped are close to where we have done the field work, and it can be established that they have similar properties. The last hypothesis is generally false; as we stated before, this area presents typical pan-shaped islands with perimetrical

levees and a central depression. The exact height profile of every island is unknown and very difficult to measure, but the maximum height difference between the central depression and the island border can be estimated to be 50 cm on average.

Consequently, the first order overall error in the estimation of water volume inside marshes comes from three sources: error on the SAR-based water level retrieval scheme, errors on the area determination and errors in the island depth due to incomplete knowledge about the island surface structure. Water volume inside marshes is then

$$V = Ah \tag{4}$$

where V is the volume, A the area of the patch and h the water level. Then, the volume error can be estimated as,

$$\frac{\Delta V}{V} = \frac{\Delta A}{A} + \frac{\Delta h}{h} \cong \frac{\Delta A}{A} + \frac{\Delta h_m}{h} + \frac{\Delta h_i}{h} \tag{5}$$

where the subscripts m and i corresponds to model and island error in water height determination. For patches of the size we are dealing with (>1000 pixels), the largest expected error in the area determination is ~5% (ESA, 2006). A conservative estimation of the error associated to the SAR-based water level retrieval model used is 20% (Grings et al., 2006). The last error (related with island depth uncertainties) is difficult to estimate, because we don't have a profile of the islands. The worst case is to consider a linear profile between the island border and the island center, and this leads to an error of 66% in the water volume. On the other hand, if the island was perfectly cylindrical, the expected error will be zero. Of course, these two hypotheses are unrealistic, and choosing between them will lead to a wrong estimation. As a result, the correct profile should lie between a linear and a vertical one, and so, the expected error is in the range 0–66%. A realistic but conservative estimate is around ~30%. So, the overall error estimate for the marsh water content is ~55%. This overall error is discussed in Section 8.

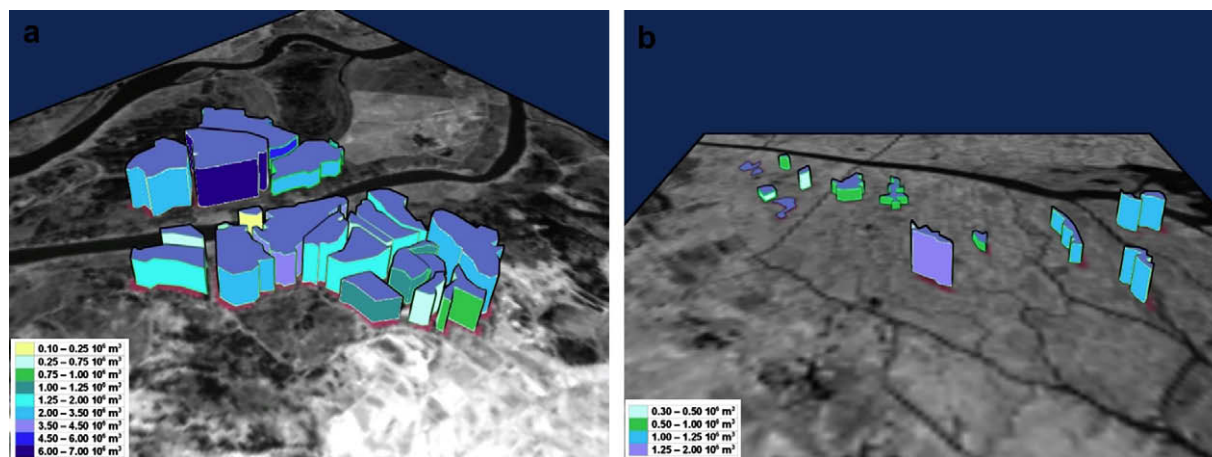


Fig. 6. Water volume inside marsh samples delimited by islands levees, superimposed on a Landsat ETM + panchromatic image (colors indicate water volume): (a) *junco* marsh samples, at both sides of the Paraná de las Palmas River and (b) *cortadera* marsh samples, at the right margin of the Paraná de las Palmas River.

8. Discussion and conclusions

Marsh water storage capacity is a very important magnitude to understand the hydrodynamical behaviour of a wetland marsh. It is the key parameter in flood control estimation, and it has to be estimated and monitored systematically, because it changes with seasons, with daily tides and even with longer cycles (i.e., El Niño phenomena). However, its direct determination remains as an open issue, since in major wetlands measurements devices in the floodplain are not available as required.

Indirect methods for marsh water storage capacity estimation can be derived from hydrodynamical information of the major rivers in the watershed. These methods make assumptions about the water level inside the marsh from the knowledge of the water level in a neighbouring river. In general, even the best assumptions used are crude, since they assume that the water level in the floodplain is the same as that in the river. Another possible method to measure marsh water storage capacity would be the use of radar remote sensing. The methods based on radar data are of course indirect methods, and use the known fact that the marsh σ^0 is influenced by the presence of surface water.

As it was described in Section 1, there are several radar-based methods available for water level estimation.

The approach proposed in this paper is able to estimate water level inside *junco* and *cortadera* marshes with an overall *rms* error of 22 cm (Grings et al., 2006). Since with ENVISAT ASAR we only observed one major flooding event, the retrieval scheme derived is only valid for water level ranges between 5 cm and 1.8 m. For lower water level, the soil is saturated but not flooded, the double bounce interaction mechanism present in the marshes is not significant and the retrieval algorithm is invalid. For higher water level, the marshes are completely flooded (underwater) and the observed σ^0 is due to surface scattering in water. The reported error in water level propagates to the marsh water storage capacity estimation, along with any uncertainties in the area determination and island bathymetry profile. Considering all the error contributions (Eq. (5)), as an overall conservative assessment, this method can estimate marsh water storage capacity in areas near places where field work has been done with a 55% error.

It is still an open issue to determine which error is acceptable for a water storage capacity retrieval algorithm. This definition is related to the use of this magnitude as an input to wetland hydrodynamical models, and it depends on the model and hypothesis used. But in any case, the large error obtained using the method proposed in this work should be compared with the reported error of other methods. The hydrodynamical approach for the estimation of marsh water storage capacity reports errors from 30% (Alsdorf, 2002) to 50% (Coe, 2000). The technique based on radar altimetry has not been used to estimate water storage, but due to the lack of reliable spatial information, the expected errors are large. InSAR techniques report errors in marsh water level as low as 7% (Alsdorf, 2002), which in the better case, leads to errors of about 10% in marsh water storage capacity. It should be noticed

that this better case ignores the errors due to island bathymetric uncertainties, which are the main sources of error in most water storage capacity estimations (see Eq. (5)). The reported value for water level estimation for the InSAR case (7%) should be compared with the overall error reported in our case (20%). But of course, the InSAR method suffers the drawbacks already mentioned; the worst of it being the low temporal resolution.

The water level retrieval method proposed in this work can be improved. One way to do this is to use the cross-polarized data (HV), already available in ENVISAT ASAR images. The HV σ^0 also changes with water level, and can be used as another constraint in the retrieval scheme. Furthermore, this method has the theoretical advantage of being able to work for all ENVISAT ASAR incidence angles, since it is based in a radiative transfer model that can simulate the marsh σ^0 for different incidence angles. The temporal window between acquisitions is greatly reduced (from 21 to 3 days) if all incidence angles are included, allowing a retrieval scheme with larger temporal resolution. Furthermore, this retrieval scheme was developed for C-band SAR data, but it also works for L-band SAR data (Grings et al., 2004). The addition of L-band data would include more constraints into the retrieval scheme, improving its accuracy.

The inclusion of cross-polarized, multiangular and multi-frequency information, could considerably reduce the water level retrieval scheme errors, thus improving the estimation of water storage capacity.

Other sources of information, in addition to radar data, are required to reduce the errors introduced by island bathymetric profile uncertainties.

References

- Alsdorf, D.E., 2002. Interferometric SAR observations of water level changes: potential targets for future repeat-pass AIRSAR missions, AIRSAR Earth Science and Application Workshop.
- Bach, H., Mauser, W., 2003. Methods and examples for remote sensing data assimilation in land surface process modelling. 1. IEEE Transactions on Geoscience and Remote Sensing 41 (7), 1629–1637.
- Bracaglia, M., Ferrazzoli, P., Guerriero, L., 1995. A fully polarimetric multiple scattering model for crops. Remote Sensing of Environment 54, 170–179.
- Coe, M.T., 2000. Modeling terrestrial hydrological systems at the continental scale: testing the accuracy of an atmospheric GCM. Journal of Climate 13, 686–704.
- ESA, 2006. ASAR Product Handbook. ESA.
- Grings, F., Ferrazzoli, P., Jacobo Berles, J.C., Karszenbaum, H., Tiffenberg, J., Kandus, P., Depine, R., 2004. Comparing capabilities of current C-band systems and future L-band Argentine SAR system in wetland studies, 4th International Symposium on Retrieval of Bio- and Geo-physical Parameters from SAR Data for Land Applications, Innsbruck, 2004.
- Grings, F.M., Ferrazzoli, P., Karszenbaum, H., Tiffenberg, J., Kandus, P., Guerriero, L., Jacobo-Berles, J.C., 2005. Temporal evolution of junco marshes radar signatures. IEEE Transactions on Geoscience and Remote Sensing 43 (10), 2238–2245.
- Grings, F.M., Ferrazzoli, P., Jacobo-Berles, J.C., Karszenbaum, H., Tiffenberg, J., Pratalongo, P., Kandus, P., 2006. Monitoring flood condition in marshes using EM models and ENVISAT ASAR observations. IEEE Transactions on Geoscience and Remote Sensing 44 (4), 936–942.

- Grings, F., Ferrazzoli, P., Karszenbaum, H., Salvia, M., Kandus, P., Jacobo Berles, J.C., Perna, P. Model investigation about the potential of C band SAR in herbaceous wetlands flood monitoring, *International Journal of Remote Sensing*, in press.
- Hess, L.L., Melack, J.M., Filoso, S., Wang, Y., 1995. Delineation of inundated area and vegetation along the Amazon floodplain with the SIR-C synthetic aperture radar. *IEEE Transactions Geoscience and Remote Sensing*. 33, 896–902.
- Junk, W.J., Bayley, P.B., Sparks, R.E., 1989. Flood pulse concept in river–floodplain systems, *Proceedings of the international large rivers symposium*, Dodge, 110–127.
- Kandus, P., 1997. Análisis de los patrones de vegetación a escala regional en el Bajo Delta del Río Paraná (Argentina). Ph.D. Dissertation, Universidad de Buenos Aires, Buenos Aires, Argentina.
- Kandus, P., Málvarez, A.I., Madanes, N., 2003. Study on the herbaceous plant communities in the lower delta islands of the Paraná river (Argentina). *Darwiniana* 41 (1–4), 1–16.
- Karszenbaum, H., Kandus, P., Martinez, J.M., Le Toan, T., Tiffenberg, J. and Parmuchi, G., 2000. ERS-2, RADARSAT SAR backscattering characteristics of the Paraná River Delta wetlands, Argentina, *ERS-Envisat Symposium (ESA)*, ESA-SP-461, 2000.
- Kasischke, E.S., Smith, K.B., Bourgeau-Chavez, L.L., Romanowicz, E.A., Brunzell, S., Richardson, C.J., 2003. Effects of the seasonal hydrologic patterns in South Florida wetlands on radar backscatter measured on ERS-2 SAR image. *Remote Sensing of Environment* 88, 423–441.
- Keddy, P.A., 2002. *Wetland Ecology*. Cambridge University Press.
- Parmuchi, M.G., Karszenbaum, H., Kandus, P., 2002. Mapping the Paraná River Delta wetland using multitemporal RADARSAT/SAR data and a decision based classifier. *Canadian Journal of Remote Sensing* 28, 631–635.
- Pope, K.O., Rejmankova, E., Paris, F.F., Woodruff, R., 1997. Detecting seasonal flooding cycles in marshes of the Yucatan peninsula with SIR-C polarimetric radar imagery. *Remote Sensing of Environment* 59, 157–166.
- Pratolongo, P., 2005. Dinámica de comunidades herbáceas del Bajo Delta del río Paraná sujetas a diferentes regímenes hidrológicos y su monitoreo mediante sensores remotos. Ph.D. Dissertation, Universidad de Buenos Aires, Buenos Aires, Argentina.
- Richey, J.E., Mertes, L.A.K., Dunne, T., Victoria, R.L., Forsberg, B.R., Tancredi, A.C.N.S., Oliveira, E., 1989. Sources and routing of the Amazon River flood wave. *Global Biogeochemical Cycles* 3, 191–204.
- Sang-Wan, Kim, Wdowinski, S., Amelung, F., Dixon, T.H., 2005. C-band interferometric SAR measurements of water level change in the wetlands: examples from Florida and Louisiana, *International Geoscience and Remote Sensing Symposium, 2005 (IGARSS'05)*. *Proceedings 2005 IEEE International* 4, July 25–29, 2005, pp. 2708–2710.